# Supporting Information

Novel high-pressure phases of nitrogen-rich Y-N compounds

Shuang Liu, Dan Xu, Ran Liu, Zhen Yao* and Peng Wang*

State Key Laboratory of Superhard Materials, College of Physics, Jilin University, Changchun 130012, P.R.China.

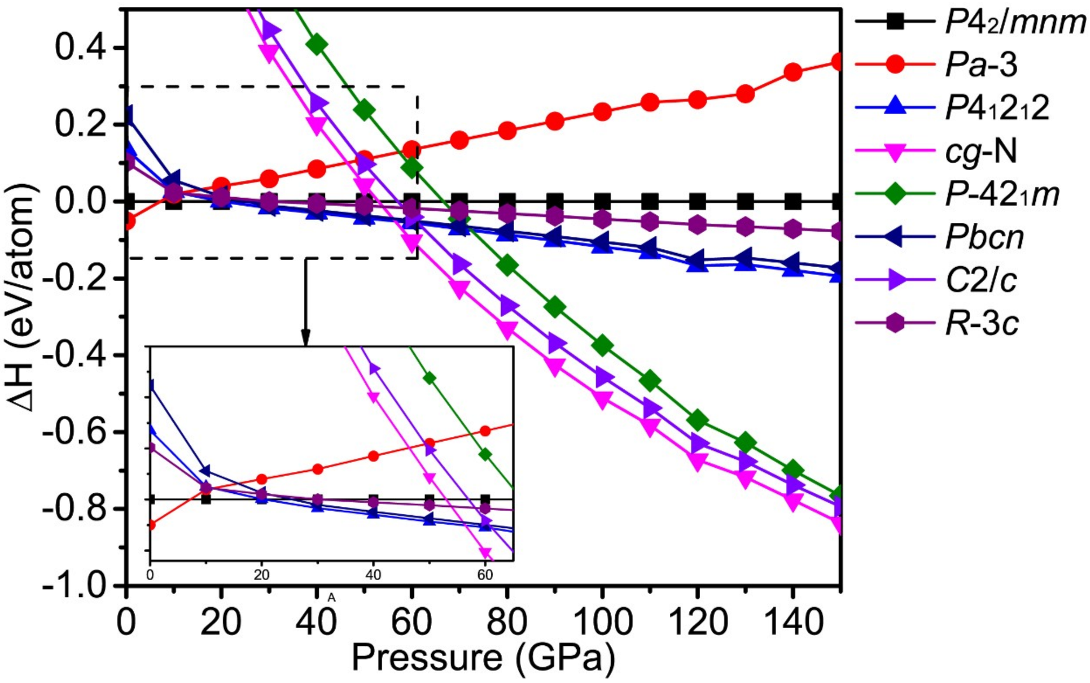


Fig.S1. Enthalpy-pressure diagrams of various nitrogen phases at 0-150 GPa.

* Corresponding author.
E-mail address: yaozhen@jlu.edu.cn
E-mail address: wangpengtrrs@jlu.edu.cn

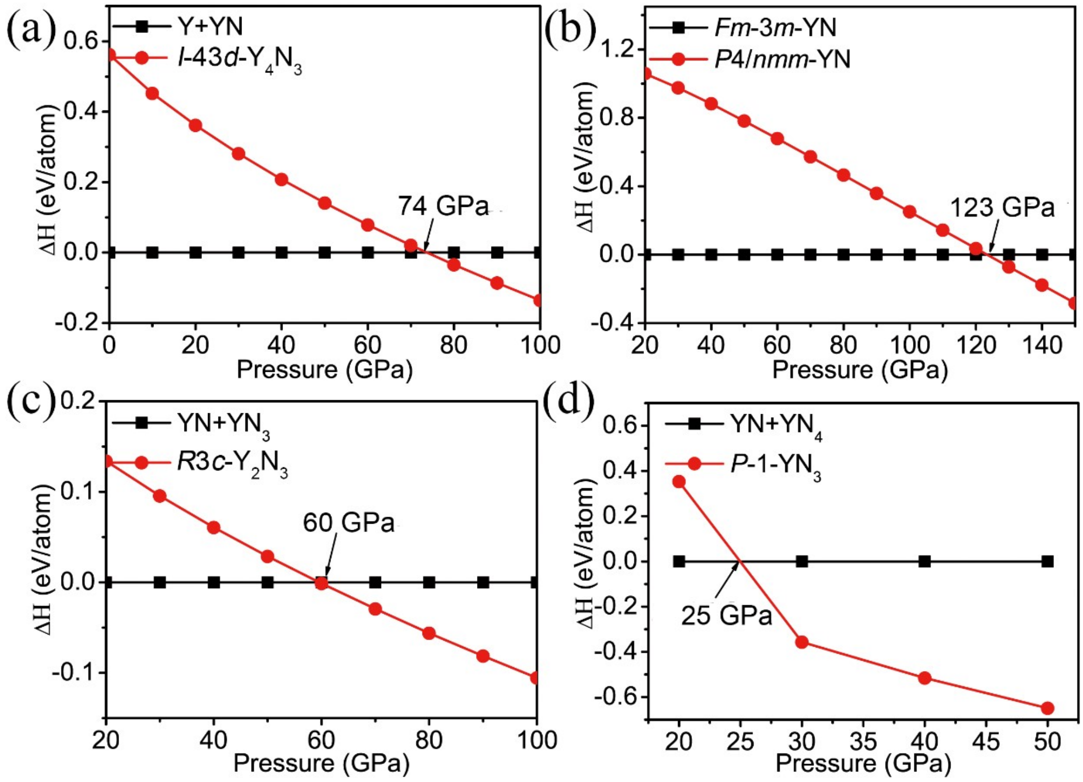


**Figure.S2.** Enthalpy-pressure diagrams of $Y_4N_3$ (a), YN (b), $Y_2N_3$ (c) and $YN_3$ (d).

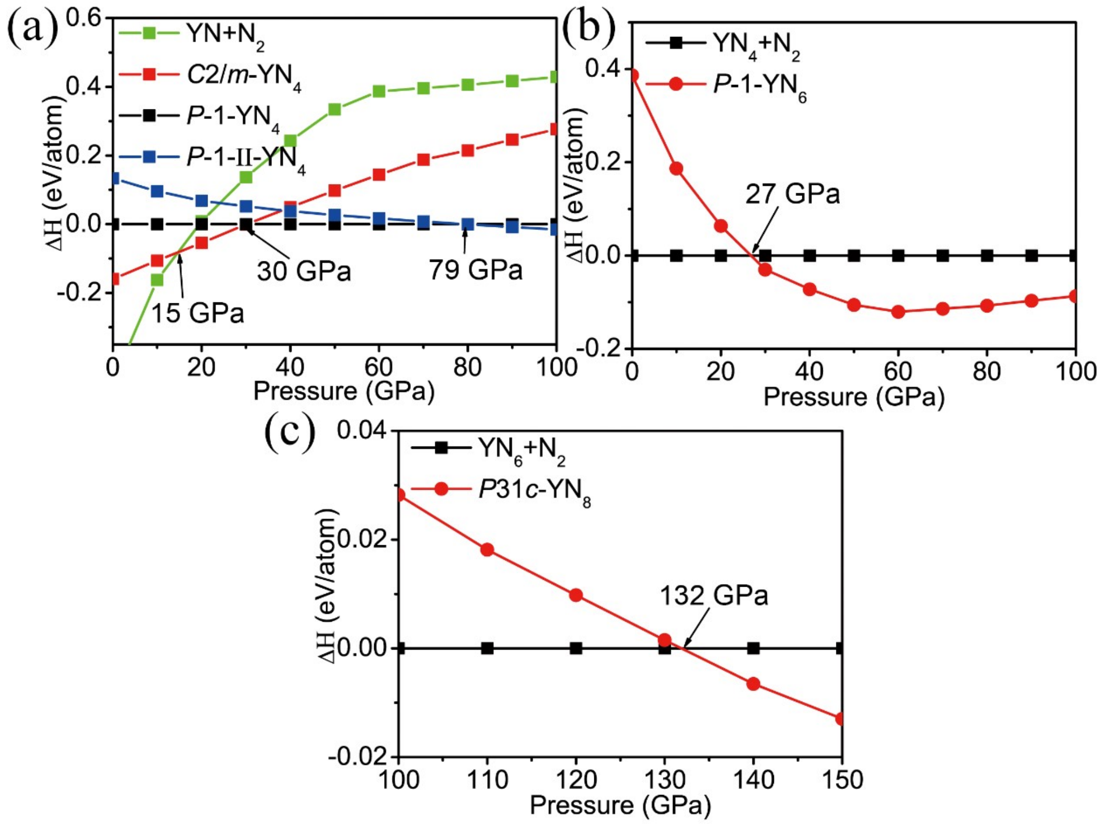


**Figure.S3.** Enthalpy-pressure diagrams of $YN_4$ (a), $YN_6$ (b) and $YN_8$ (c).

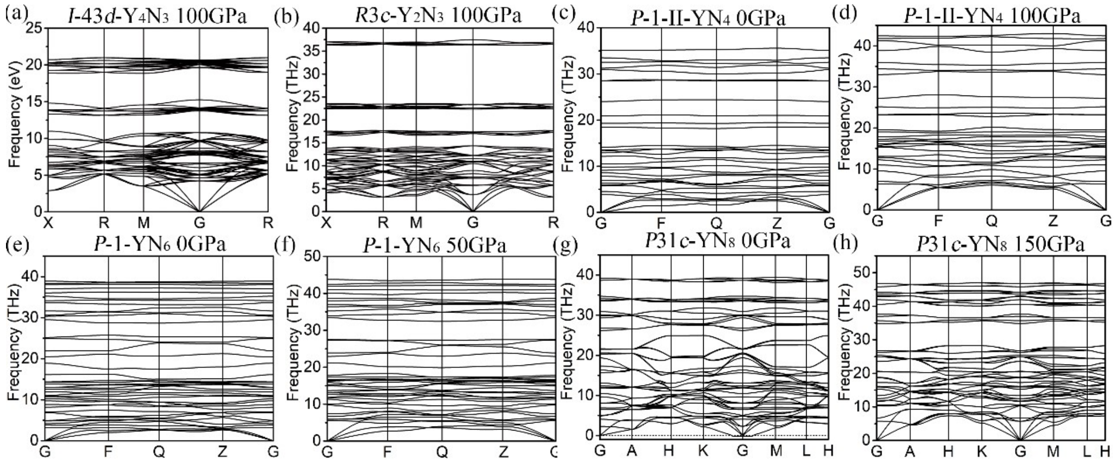


**Figure.S4.** The phonon dispersion curves for (a) *I*-43*d*-$Y_4N_3$ phase at 100 GPa; (b) *R*3*c*-$Y_2N_3$ phase at 100 GPa; (c) *P*-1-II-$YN_4$ at 0 GPa; (d) *P*-1-II-$YN_4$ at 100 GPa; (e) *P*-1-$YN_6$ at 0 GPa; (f) *P*-1-$YN_6$ at 50 GPa; (g) *P*31*c*-$YN_8$ at 0 GPa; and (h) *P*31*c*-$YN_8$ at 150 GPa.

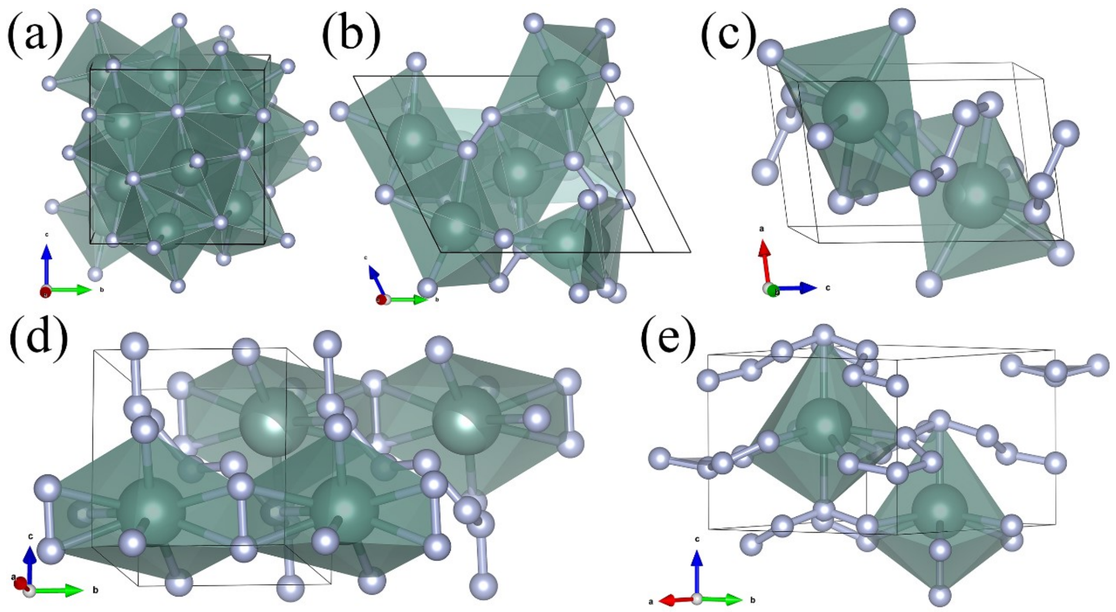


**Figure.S5.** The polyhedral structures of predicted Y-N compounds: (a) *I*-43*d*-$Y_4N_3$ phase at 100 GPa; (b) *R*3*c*-$Y_2N_3$ phase at 100 GPa; (c) *P*-1-II-$YN_4$ phase at 100 GPa; (d) *P*-1-$YN_6$ phase at 50 GPa and (e) *P*31*c*-$YN_8$ phase at 150 GPa. The green and white spheres denote Y and nitrogen atoms, respectively.

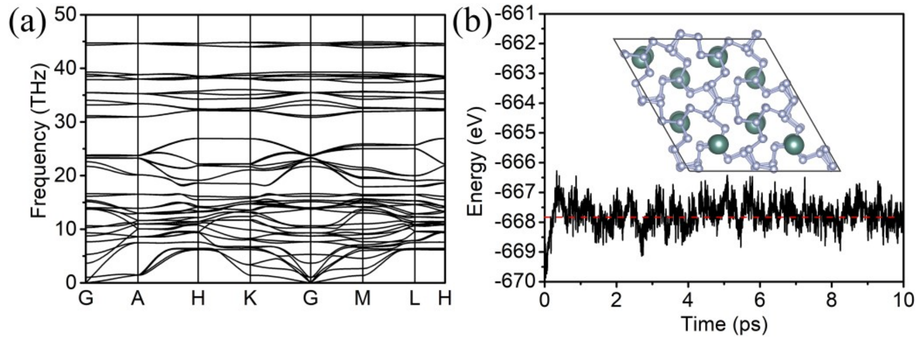


**Figure.S6.** The phonon dispersion curves for $P31c$-$YN_8$ at 60 GPa (a); fluctuations of total energies and snapshots of $P31c$-$YN_8$ at 60 GPa (b).

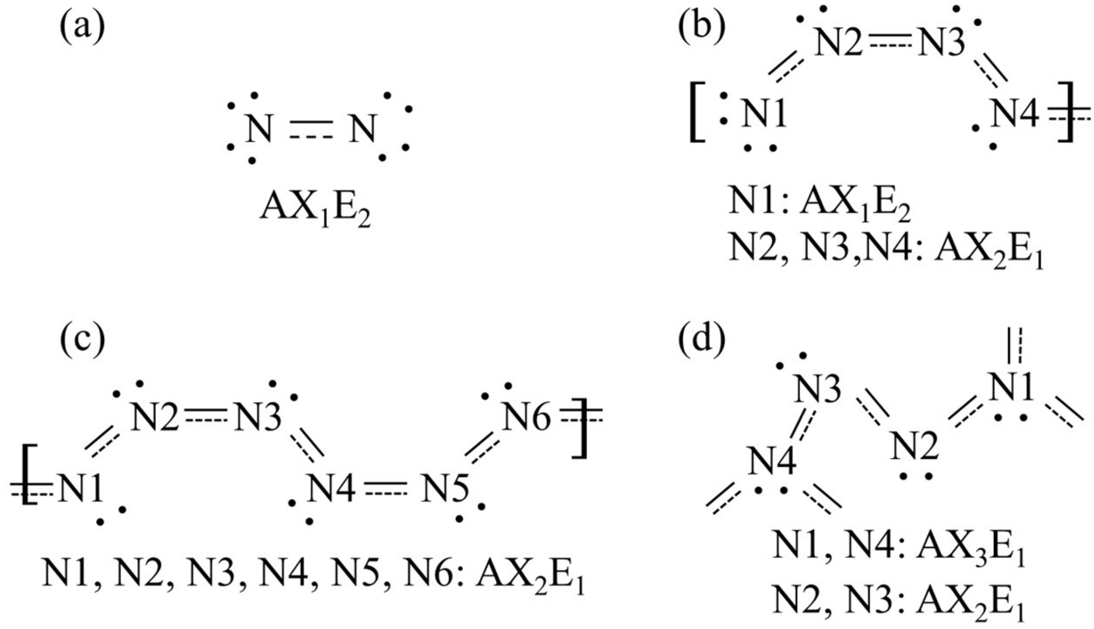


**Figure.S7** Lewis structure for the periodic unit of the (a) $R3c$-$Y_2N_3$, (b) $P$-1-II-$YN_4$, (c) $P$-1-$YN_6$, and (d) $P31c$-$YN_8$.

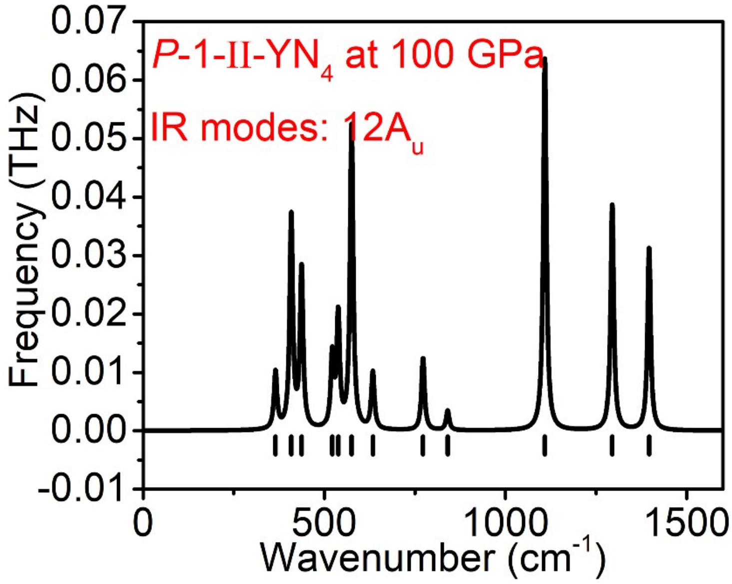


**Figure.S8** The IR spectrum of *P*-1-II-$YN_4$ at 100 GPa.

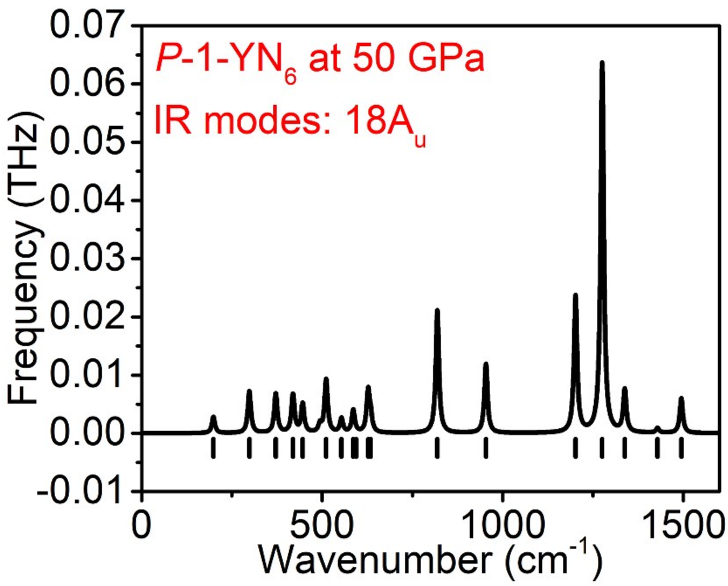


**Figure.S9** The IR spectrum of *P*-1-$YN_6$ at 50 GPa.

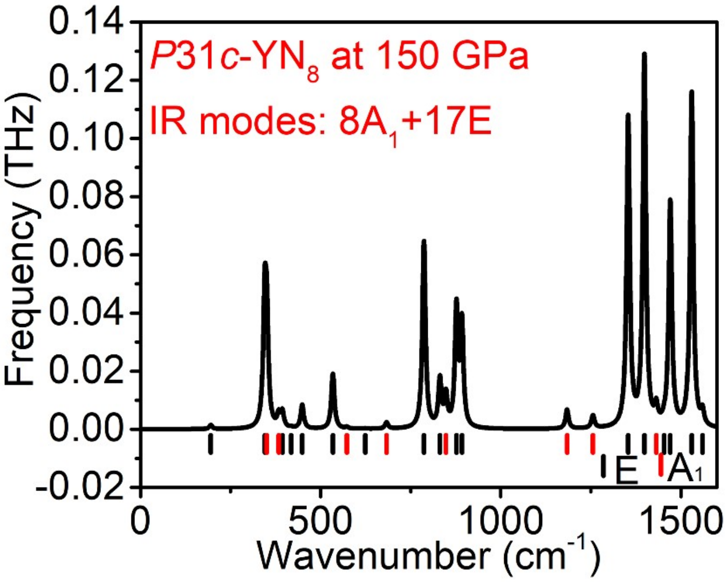


**Figure.S10** The IR spectrum of $P31c$-$YN_8$ at 150 GPa.

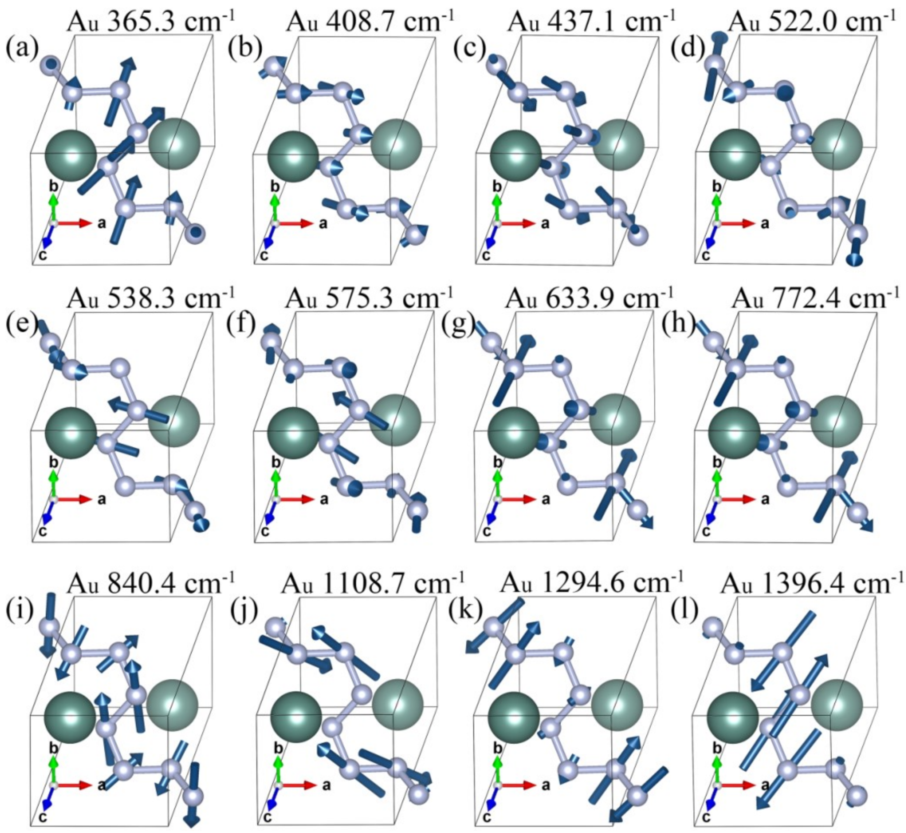


**Figure.S11.** IR active images of $P$-1-II-$YN_4$.

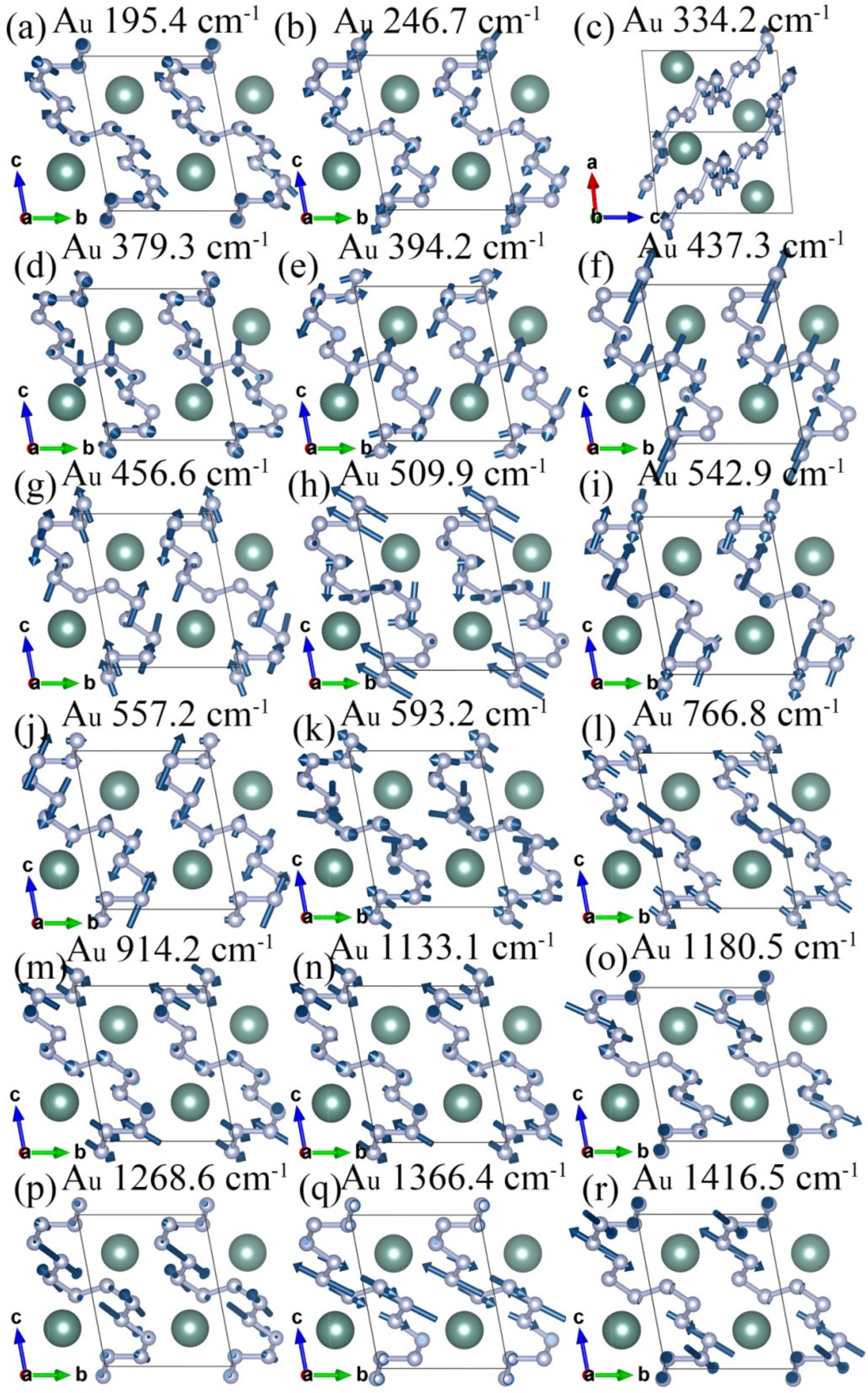


**Figure.S12.** IR active images of *P*-1-$YN_6$.

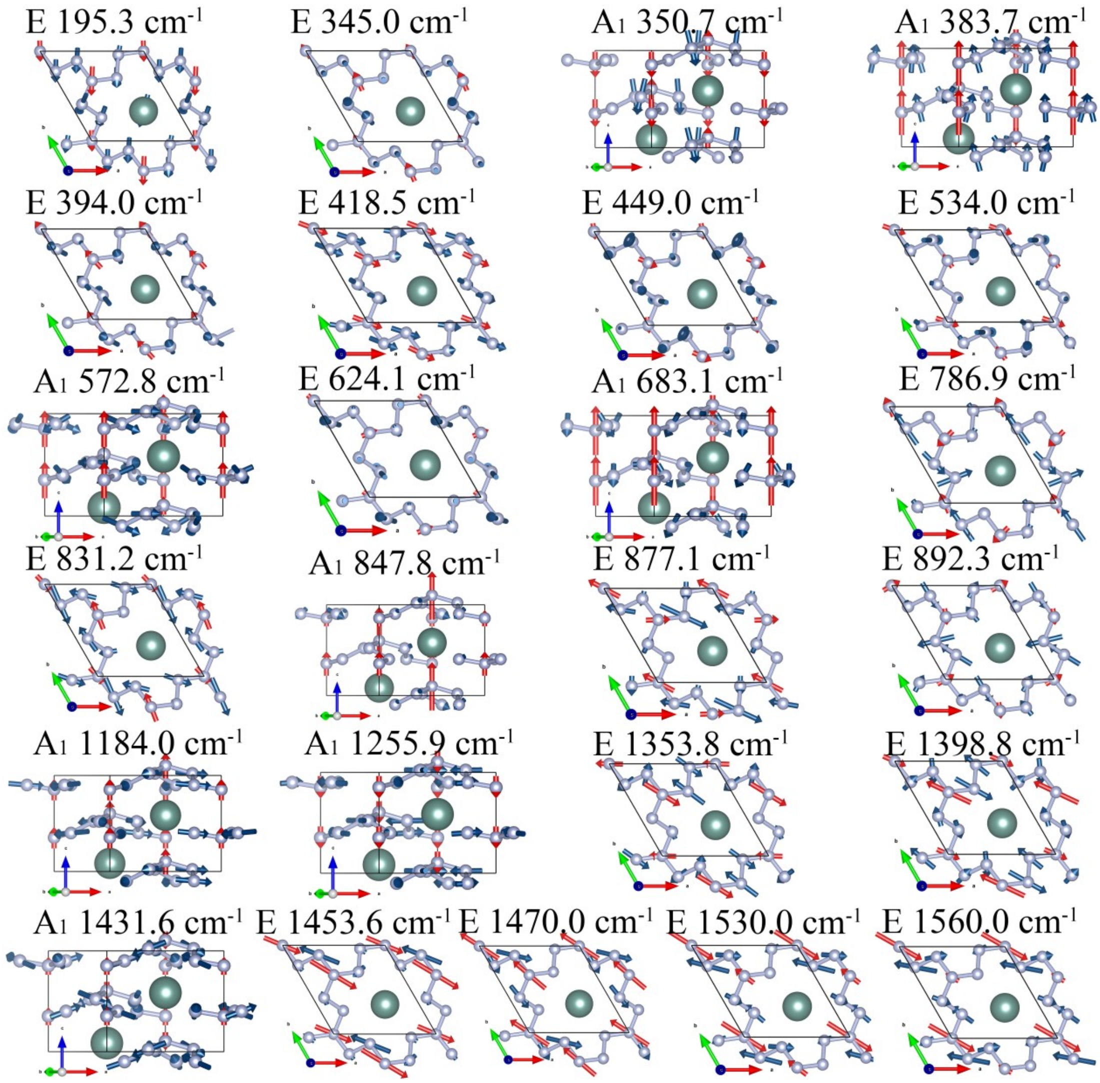


**Figure.S13.** IR active images of *P*31*c*-$YN_8$.

**Table S1.** Elastic tensor $C_{ij}$ (in GPa) of cubic *I*-43*d*-$Y_4N_3$:

| $C_{ij}$ | 1 | 2 | 3 | 4 | 5 | 6 |
|---|---|---|---|---|---|---|
| 1 | 745.323 | 207.651 | 207.663 | 0.029 | 0.032 | 0.037 |
| 2 | 207.651 | 745.318 | 207.654 | 0.030 | 0.043 | 0.030 |
| 3 | 207.663 | 207.654 | 745.328 | 0.026 | 0.032 | 0.039 |
| 4 | 0.029 | 0.030 | 0.026 | 147.480 | 0.009 | 0.009 |
| 5 | 0.032 | 0.043 | 0.032 | 0.009 | 147.476 | 0.002 |
| 6 | 0.037 | 0.030 | 0.039 | 0.009 | 0.002 | 147.467 |

**Table S2.** Elastic tensor $C_{ij}$ (in GPa) of rhombohedral *R*3*c*-$Y_2N_3$:

| $C_{ij}$ | 1 | 2 | 3 | 4 | 5 | 6 |
|---|---|---|---|---|---|---|
| 1 | 705.652 | 271.457 | 323.263 | -72.511 | 0.000 | 0.000 |
| 2 | 271.457 | 705.652 | 323.263 | 72.511 | 0.000 | 0.000 |
| 3 | 323.263 | 323.263 | 793.240 | 0.000 | 0.000 | 0.000 |

| | | | | | | |
|---|---|---|---|---|---|---|
| 4 | -72.511 | 72.511 | 0.000 | 270.018 | 0.000 | 0.000 |
| 5 | 0.000 | 0.000 | 0.000 | 0.000 | 270.018 | -72.511 |
| 6 | 0.000 | 0.000 | 0.000 | 0.000 | -72.511 | 217.097 |

**Table S3.** Elastic tensor $C_{ij}$ (in GPa) of triclinic *P*-1-II-$YN_4$:

| $C_{ij}$ | 1 | 2 | 3 | 4 | 5 | 6 |
|---|---|---|---|---|---|---|
| 1 | 626.629 | 242.375 | 266.719 | -7.653 | 8.49 | -8.186 |
| 2 | 242.375 | 996.54 | 245.267 | -31.671 | -31.073 | 77.867 |
| 3 | 266.719 | 245.267 | 695.532 | -7.591 | -83.248 | -15.114 |
| 4 | -7.653 | -31.671 | -7.591 | 196.406 | 10.225 | -61.593 |
| 5 | 8.49 | -31.073 | -83.248 | 10.225 | 211.865 | 10.118 |
| 6 | -8.186 | 77.867 | -15.114 | -61.593 | 10.118 | 217.043 |

**Table S4.** Elastic tensor $C_{ij}$ (in GPa) of triclinic *P*-1-$YN_6$:

| $C_{ij}$ | 1 | 2 | 3 | 4 | 5 | 6 |
|---|---|---|---|---|---|---|
| 1 | 599.118 | 252.695 | 177.616 | -71.517 | 10.015 | -24.61 |
| 2 | 252.695 | 386.018 | 219.506 | -120.224 | -13.156 | 51.382 |
| 3 | 177.616 | 219.506 | 347.887 | 47.762 | 28.918 | -8.231 |
| 4 | -71.517 | -120.224 | 47.762 | 185.717 | -10.785 | -20.54 |
| 5 | 10.015 | -13.156 | 28.918 | -10.785 | 89.277 | -81.411 |
| 6 | -24.61 | 51.382 | -8.231 | -20.54 | -81.411 | 173.399 |

**Table S5.** Elastic tensor $C_{ij}$ (in GPa) of trigonal *P*31*c*-$YN_8$:

| $C_{ij}$ | 1 | 2 | 3 | 4 | 5 | 6 |
|---|---|---|---|---|---|---|
| 1 | 1158.402 | 253.814 | 304.103 | 0.000 | -60.767 | 0.000 |
| 2 | 253.814 | 1158.402 | 304.103 | 0.000 | 60.767 | 0.000 |
| 3 | 304.103 | 304.103 | 845.926 | 0.000 | 0.000 | 0.000 |
| 4 | 0.000 | 0.000 | 0.000 | 140.746 | 0.000 | 60.767 |
| 5 | -60.767 | 60.767 | 0.000 | 0.000 | 140.746 | 0.000 |
| 6 | 0.000 | 0.000 | 0.000 | 60.767 | 0.000 | 452.294 |

The mechanical stability criteria of cubic structure shown as follows:
$C_{11}$-$C_{12}$>0;
$C_{11}$+2$C_{12}$>0;
$C_{44}$>0.

The cubic *I*-43*d*-$Y_4N_3$ is mechanically stable due to their elastic tensor $C_{ij}$ satisfy to all the criteria.

The mechanical stability criteria of tetragonal structure shown as follows:
$C_{11}>|C_{12}|$;
$2C_{13}C_{13}<C_{33}(C_{11}+C_{12})$;
$C_{44}$>0.

The rhombohedral $R3c$-$Y_2N_3$ is mechanically stable due to their elastic tensor $C_{ij}$ satisfy to all the criteria.

The mechanical stability criteria of monoclinic/triclinic structure shown as follows:

$C_{11}>0$

$C_{22}>0$

$C_{33}>0$

$C_{44}>0$

$C_{55}>0$

$C_{66}>0$

$[C_{11}+C_{22}+C_{33}+2(C_{12}+C_{13}+C_{23})]>0$

$(C_{33}C_{55}-C_{35}C_{35})>0$

$(C_{44}C_{66}-C_{46}C_{46})>0$

$(C_{22}+C_{33}-2C_{23})>0$

$(C_{22}(C_{33}C_{55}-C_{35}C_{35})+2C_{23}C_{25}C_{35}-C_{23}C_{23}C_{55}-C_{25}C_{25}C_{33})>0(2(C_{15}C_{25}(C_{33}C_{12}-C_{13}C_{23})+C_{15}C_{35}(C_{22}C_{13}-C_{12}C_{23})+C_{25}C_{35}(C_{11}C_{23}-C_{12}C_{13}))-(C_{15}C_{15}(C_{23}C_{33}-C_{23}C_{23})+C_{25}C_{25}(C_{11}C_{33}-C_{13}C_{13})+C_{35}C_{35}(C_{11}C_{22}-C_{12}C_{12}))+C_{55}g)>0$

$g=C_{11}C_{22}C_{33} - C_{11}C_{23}C_{23} - C_{22}C_{13}C_{13} - C_{33}C_{12}C_{12} + 2C_{12}C_{13}C_{23}$

The triclinic $P$-1-II-$YN_4$ and triclinic $P$-1–$YN_6$ are mechanically stable due to their elastic tensor $C_{ij}$ satisfy to all the criteria.

The mechanical stability criteria of trigonal structure shown as follows:

$C_{11}>|C_{12}|$;

$C_{13}C_{13}<0.5C_{33}(C_{11}+C_{12})$;

$C_{14}C_{14}<0.5C_{44}(C_{11}-C_{12})$;

$C_{44}>0$.

The trigonal $P31c$-$YN_8$ is mechanically stable due to their elastic tensor $C_{ij}$ satisfy to all the criteria.

**Table S6.** Crystal structure parameters for Y-N compounds.

| Compounds | Pressure (GPa) | Space Group | Lattice Parameters | Wyckoff Positions | | | |
|---|---|---|---|---|---|---|---|
| $Y_4N_3$ | 100 | *I*-43*d* | a=b=c=6.6724 | Y1 | 0.4334 | 0.9334 | 0.5666 |
| | | | α=β=γ=90° | N1 | 0.75 | 0.125 | 0.0000 |
| $Y_2N_3$ | 100 | *R*3*c* | a=b=10.1362,c=6.2071 | Y1 | 0.2308 | 0.3653 | 0.4145 |
| | | | α=β=90°,γ=120° | Y2 | 0.0000 | 0.0000 | 0.4526 |
| | | | | N1 | 0.0736 | 0.1766 | 0.6958 |
| | | | | N2 | 0.2302 | -0.098 | 0.5688 |
| $YN_4$ | 100 | *P*-1-II | a=3.9200,b=4.0558,c=4.9745 | Y1 | 0.7804 | 0.2528 | 0.2176 |

| | | | | | | | |
|---|---|---|---|---|---|---|---|
| | | | α=93.2471°,β=111.7120°,γ=96.9587° | N1 | 0.9301 | 0.2129 | 0.7158 |
| | | | | N2 | 0.3940 | 0.3649 | 0.5125 |
| | | | | N3 | 0.4154 | 0.8019 | 0.2859 |
| | | | | N4 | 0.8253 | 0.7466 | 0.0186 |
| $YN_6$ | 50 | *P*-1 | a=3.7918,b=5.2520,c=5.9531 | Y1 | 0.8000 | 0.7188 | 0.2504 |
| | | | α=99.2457°,β=91.7902°,γ=110.7240° | N1 | 0.8061 | 0.6235 | 0.8140 |
| | | | | N2 | 0.5646 | 0.3011 | 0.4180 |
| | | | | N3 | 0.3440 | 0.9681 | 0.9352 |
| | | | | N4 | 0.3655 | 0.8708 | 0.4682 |
| | | | | N5 | 0.7777 | 0.8059 | 0.6917 |
| | | | | N6 | 0.8572 | 0.2927 | 0.0644 |
| $YN_8$ | 150 | *P*31*c* | a=52216,b=5.2216,c=4.4949 | Y1 | 0.6667 | 0.3333 | 0.5845 |
| | | | α=β=90°,γ=106.1348° | N1 | 0.2630 | 0.2242 | 0.9009 |
| | | | | N2 | 0.7005 | 0.5905 | 0.0216 |
| | | | | N3 | 0.6667 | 0.3333 | 0.1030 |
| | | | | N4 | 0.0000 | 0.0000 | 0.8526 |